Ceramics International 46 (2020) 25299–25305

Contents lists available at ScienceDirect

Ceramics International

journal homepage: www.elsevier.com/locate/ceramint

Glass powders and reactive silicone binder: Application to digital light processing of bioactive glass-ceramic scaffolds

Hamada Elsayed[a,b], Martiniano Picicco[c], Arish Dasan[d], Jozef Kraxner[d], Dusan Galusek[d,e], Enrico Bernardo[a,*]

[a] Department of Industrial Engineering, Università degli Studi di Padova, Padova, Italy
[b] Ceramics Department, National Research Centre, Cairo, Egypt
[c] Centro de Tecnología de recursos Minerales y Cerámica (CETMIC), Gonnet (La Plata), Argentina
[d] FunGlass – Centre for Functional and Surface Functionalized Glass, Alexander Dubček University of Trenčín, Trenčín, Slovakia
[e] Joint Glass Centre of the IIC SAS, TnUAD, and FChFT STU, Trenčín, Slovakia

ARTICLE INFO

Keywords:
3D bioactive glass-ceramics scaffolds
Polymer-derived ceramics
Additive manufacturing
Stereolithography

ABSTRACT

Powdered 'silica-defective glasses', mixed with silicones, have been already shown as a promising solution for the sintering, in air, of glass-ceramics with complex geometries. A fundamental advantage of the approach is the fact silicones act as binders up to the firing temperature, at which they transform into silica. A specified 'target' glass-ceramic formulation is achieved through the interaction between glass powders and the binder-derived silica. The present paper is dedicated to the extension of the approach to the digital light processing of reticulated glass-ceramic scaffolds, for tissue engineering applications, starting from glass powders suspended in an engineered photocurable silicone-based binder. The silicone component, besides providing an extended binding action up to the maximum firing temperature, stabilizes the 3D-printed shapes during sintering. The formation of a rigid silica skeleton, from the transformation of the silicone binder, prevents from excessive viscous flow of softened glass. The final phase assemblage does not depend simply on glass devitrification but also on the glass/silica skeleton interaction.

1. Introduction

Stereolithography of ceramics (in its variants) is a well-known additive manufacturing technology, yielding components with an extremely high resolution, owing to the selective exposure to UV or visible light of homogeneous oligomeric photocurable liquids, in which ceramic powders are suspended [1]. Compared to direct stereolithography of photocurable liquids for the fabrication of polymer components, stereolithography of ceramics is generally complicated by the scattering of light caused by ceramic particles. In addition, the burnout of the photocurable binders, after cross-linking, is delicate [2], for several reasons. Firstly, like in samples from other green ceramic bodies with high polymeric content (e.g. from powder injection molding), the degradation of organic matter in the debinding step, from the bulk, may be slower than at the surface; the completion of the degradation, during subsequent sintering, generates gasses, in turn leading to pores and cracks [3]. Secondly, owing to the limited packing, powders with no binder may slide on each other, with collapse of the printed structures, defined as 'debinding failure' in Fig. 1. The manufacturing of defect-free components consequently depends on the optimization of several parameters, such as granulometry of starting powders (e.g. nano-sized powders mixed with micro-sized ones) and debinding atmosphere (e.g. vacuum instead of air) [2].

Avoiding collapse or distortion of printed parts upon debinding is possible if conventional, fugitive binders are replaced by precursors which lead, upon firing, to a significant ceramic residue, in turn contributing to the final ceramic. As an example, Ti-based organometallic compounds are excellent reactive binders for TiO_2 powders, in forming nanocrystalline interparticle necks during the early stages of the sintering process [4]. The 'debinding failure', however, is not the only risk for 3D-printed components based on glass particles. The viscous flow of softened glass promotes the densification of powders at relatively low temperature, but it may also determine the coarsening and the collapse of porous structures. Uncontrolled viscous flow, in other words, may configure a 'sintering failure', as shown in Fig. 1. The flow is typically controlled by the precipitation of rigid crystal inclusions (enhancing the viscosity), in 'sinter-crystallized' glass-ceramics [5].

Silicone polymers, by offering an abundant silica-based ceramic

* Corresponding author.
E-mail address: enrico.bernardo@unipd.it (E. Bernardo).

https://doi.org/10.1016/j.ceramint.2020.06.323
Received 27 May 2020; Received in revised form 22 June 2020; Accepted 30 June 2020
Available online 08 July 2020

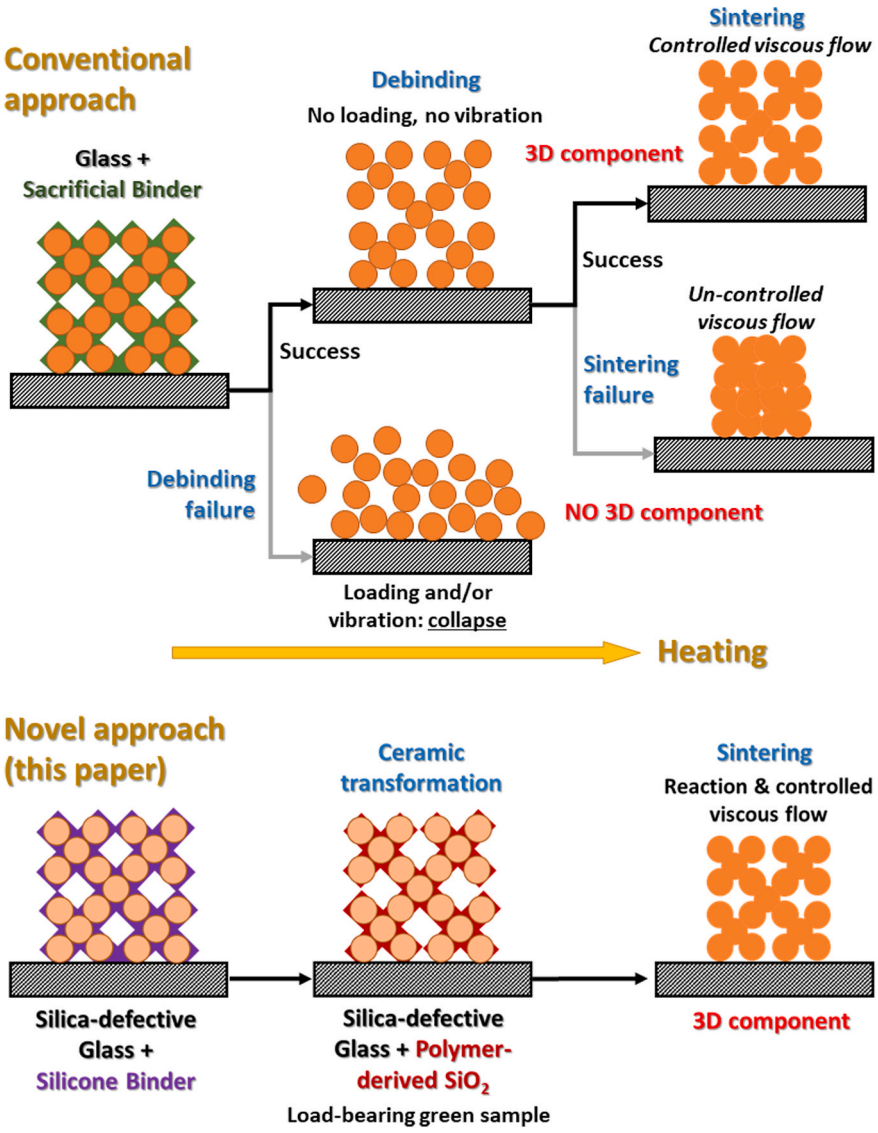

Fig. 1. Schematic representation of the overall concept of the present paper.

residue upon thermal treatment (often > 50 wt% of the starting material) [6], are particularly interesting for advanced additive manufacturing, including stereolithography [7,8]. When used to bind oxide particles, the reaction between the same particles and the ceramic residue may be variously engineered, leading to many silicate ceramics [6,8].

The adoption of glass particles, even in the presence of limited amounts of silicone binder, leads to multiform situations during firing. In particular, the incorporation of silica deriving from silicones fired in air, in the pyroplastic mass of softened glass particles, may modify the overall chemistry and the phase evolution. Changes in the overall chemistry are prevented by transforming the silica excess from the binder into a glass with a chemical composition nearly matching that of the glass particles. Ohl et al. [9], as an example - in developing translucent glass foams from a silicone resin filled with Duran® borosilicate glass powders -, realized a complete binder-powder integration by adding Na_2O and B_2O_3, both supplied in the form of borax, introduced as secondary filler. Duran® powders thus mixed with a 'Duran-like' matrix originating from the reaction between borax and silica from the oxidation of the silicone.

Changes in the phase evolution can be tuned, in glass-ceramics, also by transforming the silica excess (e.g. by introduction of secondary, reactive fillers) into silicate phases matching those from crystallization of glass powders. Zocca et al. [10], as an example, developed wollastonite-apatite glass-ceramics, with the first phase developed both by crystallization of glass and interaction between silicone and $CaCO_3$ added as an extra filler.

The present paper is aimed at presenting the successful coupling of digital light processing (DLP) of glass-ceramics with the use of a silicone reactive binder, facilitated by the simultaneous optimization of glass chemistry and binder formulation. The achievement of glass-ceramics with specified composition (referring to $CaO–Na_2O–B_2O_3–SiO_2$ system [11]) and phase assemblage is guaranteed by the use of a 'silica-defective glass' (Fig. 2), as recently proposed for the manufacturing of glass-ceramic joints for planar solid oxide fuel cell (SOFC) designs [12] and for reticulated scaffolds from direct ink writing (DIW) [13]. Changes in the chemistry of the final product are prevented by the initial modification of the chemistry of glass powders; changes in the phase evolution are prevented by the conservation of the overall chemical composition after reaction between glass and silica from the silicone matrix.

We will show that the use of a silicone binder has a specific impact also in controlling the viscous flow (preventing 'sintering failure'): the glass filler, upon softening, remains supported by the rigid silica skeleton offered by the same thermo-oxidative decomposition of the

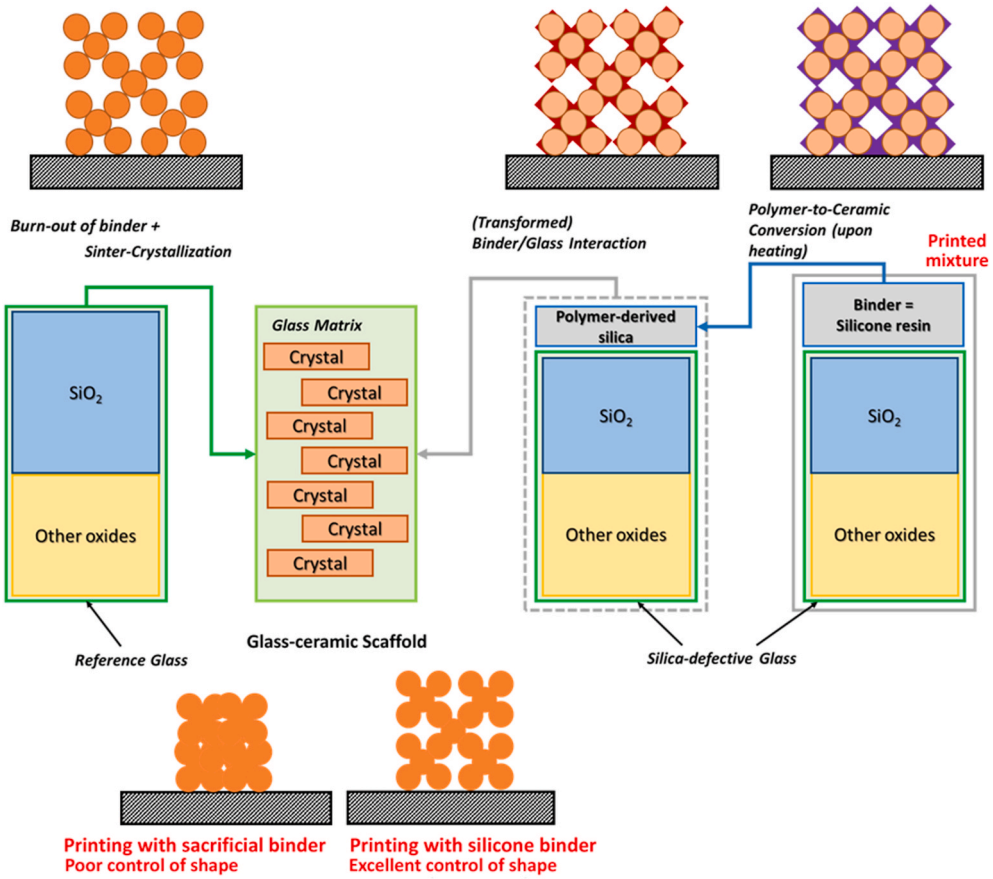

Fig. 2. Schematic representation of preparation of glass-ceramics by silicone/silica-defective glass interaction (adapted from Elsayed et al. [13]).

preceramic polymer, with excellent shape retention.

2. Experimental procedure

Table 1 reports the chemical composition of the reference glass [11], termed WB (corresponding to the molar formula ($0.05Na_2O{\cdot}0.35$ $CaO{\cdot}0.20$ $B_2O_3{\cdot}0.40$ SiO_2), and of the 'silica-defective' variant, termed WB-15. The new glass was designed to achieve the composition of the reference glass after incorporation of silica from the binder, after printing (by DLP). In particular, WB-15 was expected to yield 85 wt% of the oxides in the final product (oxide weight fraction $f_G = 0.85$), the rest being supplied by the preceramic polymer, in the form of pure silica (oxide weight fraction $f_B = 0.15$). Details on the synthesis and characterization of the two glasses are reported in our previous paper [13]. Only the particles with a diameter below 37 μm were considered.

A non-photocurable liquid silicone (H62C, Wacker-Chemie GmbH, Munich, Germany) blended with a commercial acrylate resin (available in form of oligomeric precursors, RF Resin – HT Green, Robotfactory, Mirano, Venice, Italy) was used as a preceramic polymer binder, according to the proportions presented in Table 2. The glass/silicone balance was tuned considering the silica yield of H62C (ceramic yield, $C_y = 58$ wt%) [6]. H62C liquid silicone was firstly dissolved in a limited amount of isopropyl alcohol, and then mixed with acrylate resin to form a printing solution with the silicone/solvent/resin ratio of 1:0.3:1 wt. Glass powders were mixed into the printing solution for a solid load of ~59 wt %. The mixture comprising glass powders was homogenized by mixing at a speed of 2000 rpm/min for 10 min, using a planetary mixer (THINKY ARE-250). The printing of the glass mixture was performed by DLP printer (3DLPrinter-HD 2.0, Robotfactory S.r.l., Mirano, Venice, Italy), with a layer thickness of 50 μm with an exposure time of 5 s.

For comparison, WB glass was also considered for DLP experiments: in this case, no contribution to the final ceramic was expected from the binding resin, so that glass particles were filled in the sacrificial acrylate resin. The mixture was homogenously distributed again by means of magnetic stirring overnight, in the glass/resin ratio = 21 g/10.2 g. The specific resin did not require any addition of photo-initiator or photo-absorber to be processed.

After printing, the 3D printed structures were cleaned in isopropanol, in an ultrasonic bath for 3 min, in order to remove the uncured resin, and then dried with compressed air. To ensure full curing of polymeric binders, the structures were placed in an UV furnace

Table 1
Chemical compositions (in oxides) of starting materials.

		Silica-defective glass WB-15 (wt%)	Silicone-derived residue (wt %)	Oxide distribution WB-15-silicone mixture	Reference glass WB (wt%)
Oxide	SiO_2	29.4	100	$(29.4{\cdot}f_G) + (100{\cdot}f_B) = 40$	40
	CaO	37.7		$37.7{\cdot}f_G = 32$	32
	B_2O_3	27.1		$27.1{\cdot}f_G = 23$	23
	Na_2O	5.9		$5.9{\cdot}f_G = 5$	5
Weight fractions in glass-silicone mixture		*0.85* ($= f_G$)	*0.15* ($= f_B$)		

Table 2
Formulations of glass/binder batches.

Formulation (weight proportions)		WB glass	Fugitive binder (RF Resin – HT Green)	Silicone resin (H62C)	WB-15 glass
GC#0	*Starting mix*	100	48.6		
Reference glass-ceramic	*Above 550°C*	100	0		
GC#1	*Starting mix*		25.9	25.9	85
Glass-ceramic from glass-silicone mixture	*Above 550°C*		0	15 (=25.9·C_y)	85

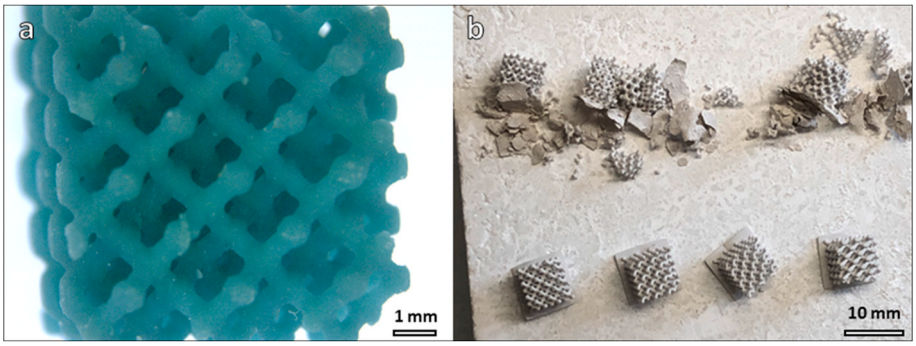

Fig. 3. a) GC#1 in the as printed state; b) GC#0 (top) and GC#1 (bottom) after treatment at 550 °C.

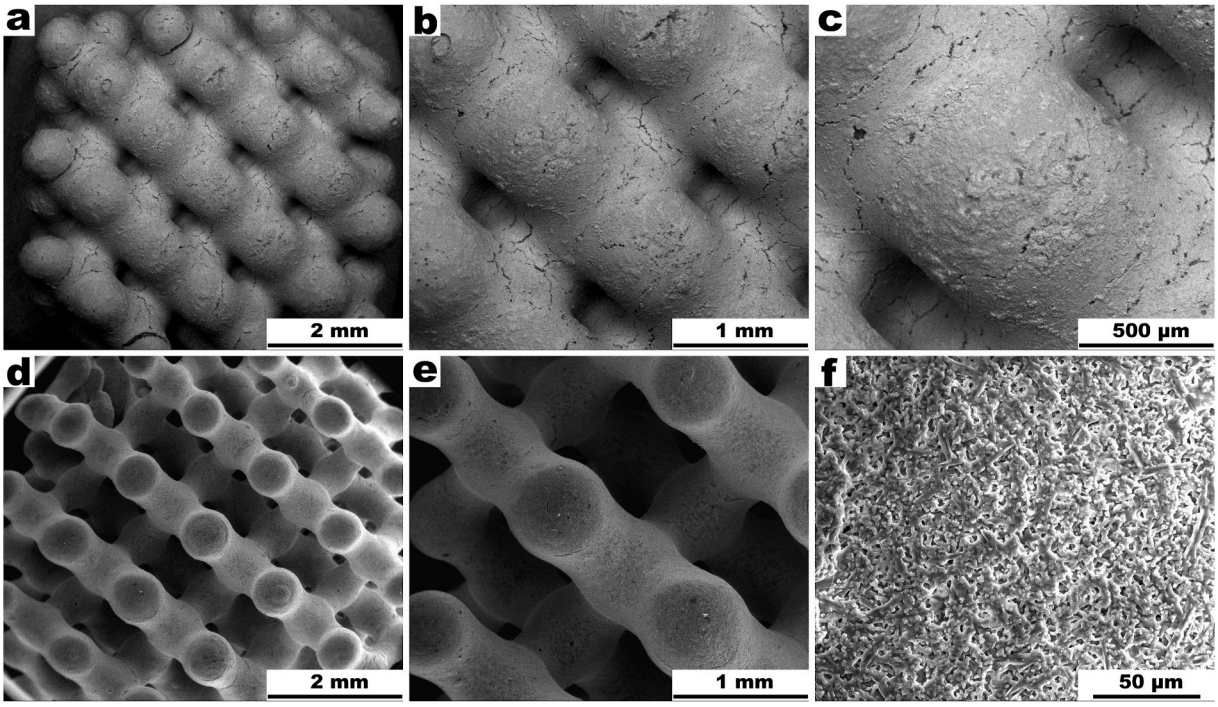

Fig. 4. SEM images of 3D glass-ceramic scaffolds (diamond-like lattice structure) obtained by DLP, after firing: a-c) GC#0 (WB glass, printed by using a sacrificial binder); d-f) GC#1 (WB-15 glass + H62C + acrylate resin).

(365 nm, Robotfactory S.r.l., Venice, Italy) and treated for an additional 15 min. Finally, the structures were heated with 0.5 °C/min to 550 °C with a holding time of 5 h and then subjected to a two-step sintering treatment, with 1 h at 700 °C and 1 h at 800 °C. The applied heating rate was 5 °C/min and natural cooling occurred after the final holding stage at 800 °C.

The obtained scaffolds were subjected to morphological analysis, using optical stereomicroscopy (AxioCam ERc 5s Microscope Camera, Carl Zeiss Microscopy, Thornwood, New York, USA) and scanning electron microscopy (FEI Quanta 200 ESEM, Eindhoven, the Netherlands), as well as to mineralogical analysis (X-ray diffraction, XRD, performed on powdered samples, with the use of Bruker AXS D8 Advance, Karlsruhe, Germany powder diffractometer). A semi-automatic phase identification was conducted by the Match! program package (Crystal Impact GbR, Bonn, Germany), supported by data from PDF-2 database (ICDD-International Centre for Diffraction Data, Newtown Square, PA). The weight proportions between crystal phases were estimated by application of Reference Intensity Ratio method [14], according to the same Match! Software.

The apparent and true densities of scaffold samples were measured with the use of a helium gas pycnometer (Micromeritics AccuPyc 1330, Norcross, GA), operating on samples in bulk (3D printed scaffold) and powder forms. The density of the ceramized scaffolds was measured geometrically using a digital calliper and by weighing them with an analytical balance. The compressive strength was evaluated at room temperature, with the use of an Instron 1121 UTM (Instron Danvers,

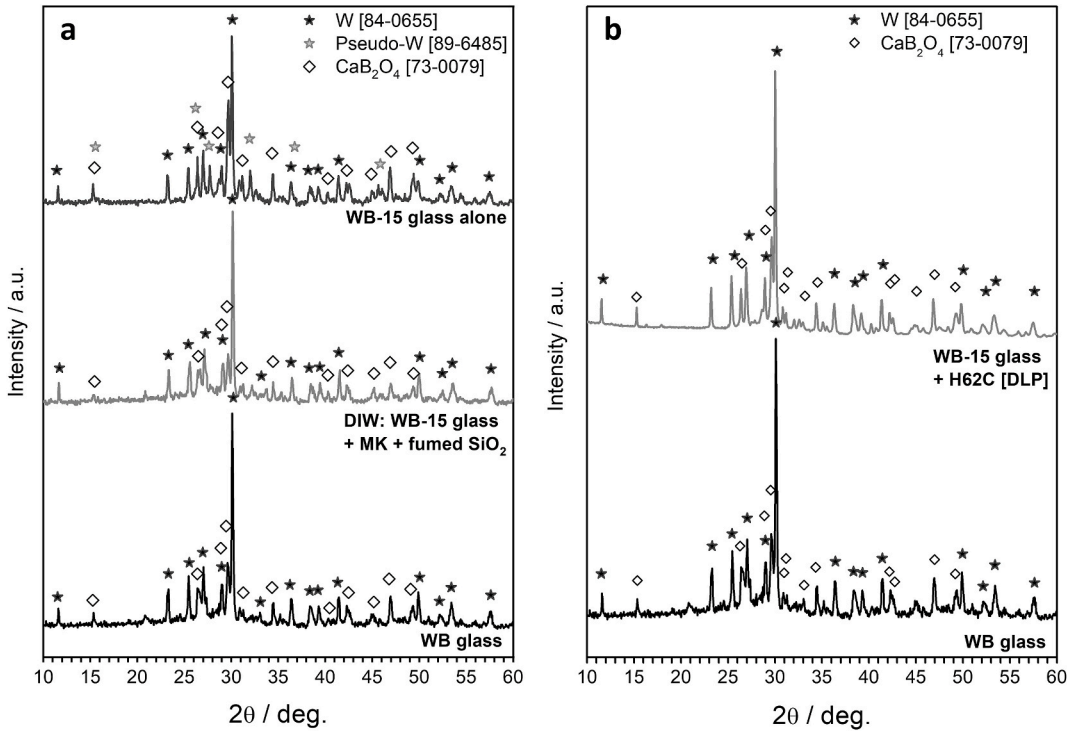

Fig. 5. Comparison between glass-ceramics from WB glass, WB-15 glass alone and WB-15 glass combined with preceramic polymers: a) previous experiments with direct ink writing (DIW) using MK silicone polymer [13]; b) present investigation (DLP using H62C silicone polymer).

MA) operating at a crosshead speed of 0.5 mm/min. Each data point represents the average value of at least 10 individual tests.

3. Results and discussion

The as-printed samples, for all formulations, were homogeneous and defect-free (Fig. 3). No particular changes could be observed passing from the reference glass WB, printed by using a fully sacrificial binder, to the silica-defective glass WB-15, printed by using silicone-based binder mixture. The latter system confirms the 'miscibility' of H62C silicone (a methyl-phenyl polysiloxane) with commercial photocurable acrylate resins [8]. With miscibility between silicones and acrylate resins we refer to the possibility of mixing the two systems at a quasi-molecular level. This mixing enables, after printing, the obtainment of uniform cellular structures, later transformed into cellular ceramics based on SiOC (by firing in N_2 atmosphere) or on phase pure crystalline silicate ceramics (by firing of mixtures containing several oxide fillers, in air) [8].

A fundamental difference among samples was observed after low temperature firing, at 550 °C, normally applied for the burn out of sacrificial binder [5]. Selected samples, in fact, were not subjected to a complete heat treatment and were extracted from the furnace after cooling to room temperature. Fig. 3b (top) shows that the sample printed from WB glass suspended in RF resin was sensitive to the above-mentioned 'debinding failure': a gentle hand pressure was sufficient to crush the samples. The structural integrity, for samples with silicone-based binder, was not compromised at all, as shown in Fig. 3b (bottom): the samples could be easily handled and, subjected to mechanical testing, exhibited a compressive strength of 0.5 ± 0.1 MPa. H62C, simply brought at the early stages of ceramic conversion [6], evidently maintained its binding action for WB-15 powders. The non-photocurable H62C silicone likely compensated the weakening effect of the burn out of RF resin with its thermally induced cross-linking [6].

Owing to the relatively large gap between dilatometric softening temperature T_d (a well-recognized threshold for significant viscous flow sintering [15]) and crystallization (~150 °C, with T_d = 654 °C, according to our previous results [13]), WB glass was expected to present a 'sintering failure' (Fig. 1), i.e. crystallization after viscous collapse of the reticulated structure (as observed with DIW experiments [13]). Fig. 4a effectively confirms the coarsening of the structure due to uncontrolled flow; in addition, as shown in Fig. 4b, the macroporosity introduced upon printing was practically sealed. Finally, WB-derived samples exhibited some cracks (Fig. 4c).

The heating conditions, after the stage at 550 °C, exactly matched those applied in the paper describing the adopted glass-ceramic system [11]. The diffraction pattern of powdered GC#0 coarsened scaffold (see Fig. 5a, bottom), sintered in the two stages at 700 and 800 °C, is nearly identical to the pattern reported in the reference paper [11], with calcium silicate (wollastonite, $CaSiO_3$, PDF#84-0655, labelled as 'W' in Fig. 5) and calcium borate (CaB_2O_4, PDF#76-0747) as the only crystalline phases.

Non-photocurable H62C, blended with photocurable acrylic resin, provided an excellent solution for developing the target phase assemblage avoiding the coarsening of printed structures observed for pure WB glass powders, as shown in Fig. 4d–f. The images at increasing magnification show that H62C-derived glass-ceramics were highly

Table 3
Estimated weight proportions between crystal phases, according to the Match! software, in fired samples.

Formulation	Starting materials	Phase (wt%)			
		W	PsW	Total $CaSiO_3$ (W + PsW)	CaB_2O_4
WB	WB glass, alone [11]	65.7	–	65.7	34.3
	WB-15/(MK + fumed silica), DIW [11]	69.6	–	69.6	30.4
	WB-15/H62C, DLP	63.0	–	63.0	37.0
WB-15	WB-15 glass, alone [11]	46.4	8.7	55.1	44.9

Table 4
Summary of physical and mechanical properties of 3D printed glass-ceramic scaffolds.

Scaffold formulation	Bulk Density, ρ (g/cm^3)	True Density, ρ' (g/cm^3)	Total porosity, vol% [rel. density, ρ_{rel} = 1-P_{tot}]	Compressive strength, σ_c (MPa)
WB-15/H62C	0.66 ± 0.07	2.70 ± 0.03	76 [ρ_{rel} = 0.24]	3.7 ± 0.4

homogeneous and crack-free.

Compared to H44 (another commercial methyl-phenyl polysiloxane, also from Wacker GmbH), H62C was known to lead to less homogeneous structures, when mixed with acrylate resin, and less phase pure silicate ceramics, in the presence of oxide fillers [8]. However, H62C was selected for better-documented exploitation as a component for biocompatible and bioactive ceramic foams [16]; in addition, we relied on extensive viscous flow of the silica defective WB-15 glass filler, promoting both mixing and reaction between the same glass and silica from the oxidation of H62C.

H62C, interacting with WB-15, effectively led to glass-ceramics with a spectacular match, in terms of phase assemblage, with the WB reference, as shown in Fig. 5b. This result is even more significant than that previously achieved operating with WB-15 'bound' by MK polymer, in pastes for direct ink writing (DIW) experiments [13], which included also highly reactive fumed silica (reported in Fig. 5a). In other words, WB-15 'recovered' the overall oxide formulation of WB (Fig. 2, Table 1) by incorporation of silica just from the silicone.

The occurrence of complex combination 'reaction-sintering-crystallization' is demonstrated also in Fig. 5. In the absence of extra silica from the binding material, WB-15 does not lead (under the same heating schedule applied to WB and WB-15/binder mixtures) to the original silicate and borate phases, with pseudo-wollastonite ($CaSiO_3$ polymorph, PDF# 89-6485, see Fig. 5a) appearing as an extra phase. In other words, the desired phase assemblage, as expected from Fig. 2, comes from the active involvement of the ceramic residue of the silicone, in the sintering and crystallization process of WB-15. The substantial equivalence between glass-ceramics from the firing of WB glass alone and from 'reaction-sintering-crystallization' (involving WB-15 glass and H62C) is confirmed by the estimated weight proportions between crystalline phases, shown in Table 3.

The mechanical properties of the obtained glass-ceramic scaffolds are reported in Table 4. According, the Gibson-Ashby model for bending-dominated open-celled foams, the compressive strength (σ_c) depends simply on the bending strength of the solid phase (σ_{bend}) and the relative density (ρ_{rel}):

$$\sigma_c = \sigma_{bend} \cdot C \cdot \rho_{rel}^{3/2} \quad \text{(Eq.1)}$$

C is a dimensionless constant (C ≈ 0.2). Reversing Eq. (1), we could estimate, from the experimental data of compressive strength and porosity, a bending strength far exceeding 100 MPa, consistent with the presence of crack-free and strong struts. In fact, these values are in good agreement with the strength reported for monolithic glass-ceramics of comparable composition [17]). More importantly, the compressive strength values are within or even above the standard reference range (2–12 MPa) of human trabecular bone [18], with a similar interconnected porosity (76 vol% for the scaffolds developed in the current work).

We believe that the presented system is just an example of a huge number of combinations between 'silica-defective' glasses and silicones to be studied in the future. Besides applying cell tests to further substantiate the equivalence of glass-ceramics from the firing of WB glass alone and from 'reaction-sintering-crystallization', we will definitely explore the method for other glass-ceramic systems, already known for excellent bioactivity and biocompatibility (e.g. Biosilicate ®) [19].

4. Conclusions

Based on the presented results the following conclusions can be drawn:

- The chemical interaction between silicone resins and glass powders, inserted as fillers, can be exploited for the manufacturing of sintered glass-ceramics with complex shapes, even by digital light processing (DLP);
- A photocurable silicone-based binder may be obtained by the simple mixing of a non-photocurable silicone with acrylate resin precursors; the silicone component provides a binding action extended up to the maximum firing temperature;
- According to the same overall chemical formulation, the firing of a reference glass (WB) as well as the firing of its 'silica-defective' variant (WB-15), reacting with silica from the binder, lead to glass-ceramics with the same phase assemblage;
- The 'silica-defective' glass (WB-15)/binder interaction leads to homogeneous and crack-free scaffolds, with excellent retention of the shape achieved by means of DLP: the specific polymer precursor evidently offers, by oxidation upon firing, a stiff silica-based network, progressively reacting with softened silica-defective glass powders.

Declaration of competing interest

The authors declare that they have no known competing financial interests or personal relationships that could have appeared to influence the work reported in this paper.

Acknowledgements

The research leading to these results has received funding from the European Union's Horizon 2020 research and innovation programme under the H2020-WIDESPREAD-01-2016-2017-TeamingPhase2 project FunGlass (Centre for Functional and Surface Functionalized Glass), grant agreement No. 739566. Discussions with Prof. A. R. Boccaccini (University of Erlangen-Nuremberg, Germany), scientific board member (Biomaterials) of the Centre for Functional and Surface Functionalized Glass, are greatly acknowledged. MP acknowledges the support of Bec.Ar Programme of the National Education Ministry of Argentina (Argentina). The authors thank Dr Johanna Eva Maria Schmidt and Ms Giada Borsoi (University of Padova) for experimental assistance.

References

[1] T. Chartier, Stereolithography of structural complex ceramic parts, J. Mater. Sci. 37 (2002) 3141–3147.
[2] H. Wu, Y. Cheng, W. Liu, R. He, M. Zhou, S. Wu, X. Song, Y. Chen, Effect of the particle size and the debinding process on the density of alumina ceramics fabricated by 3D printing based on stereolithography, Ceram. Int. 42 (2016) 17290–17294.
[3] K.S. Hwang, H.K. Lin, S.C. Lee, Thermal, solvent, and vacuum debinding mechanisms of PIM compacts, Mater. Manuf. Process. 12 (1997) 593–608.
[4] L.O. Grant, M.B. Alameen, J.R. Carazzone, C.F. Higgs III, Z.C. Cordero, Mitigating distortion during sintering of binder jet printed ceramics, Solid Freeform Fabrication 2018: Proceedings of the 29th Annual International Solid Freeform Fabrication Symposium – an Additive Manufacturing Conference, Austin, TX, USA,

Aug 2018.
[5] H. Elsayed, J. Schmidt, E. Bernardo, P. Colombo, Comparative analysis of wollastonite-diopside glass-ceramic structures fabricated via stereo-lithography, Adv. Eng. Mater. 21 (2019) 1801160.
[6] E. Bernardo, L. Fiocco, G. Parcianello, E. Storti, P. Colombo, Advanced ceramics from preceramic polymers modified at the nano-scale: a review, Materials 7 (2014) 1927–1956.
[7] J. Schmidt, P. Colombo, Digital light processing of ceramic components from polysiloxanes, J. Eur. Ceram. Soc. 38 (2018) 57–66.
[8] A. Dasan, H. Elsayed, J. Kraxner, D. Galusek, P. Colombo, E. Bernardo, Engineering of silicone-based mixtures for the digital light processing of Åkermanite scaffolds, J. Eur. Ceram. Soc. 40 (2020) 2566–2572.
[9] C. Ohl, M. Kappa, V. Wilker, F. Scheffler, M. Scheffler, Novel open-cellular glass foams for optical applications, J. Am. Ceram. Soc. 94 (2011) 436–441.
[10] A. Zocca, H. Elsayed, E. Bernardo, C.M. Gomes, M.A. Lopez-Heredia, C. Knabe, P. Colombo, J. Günster, 3D-printed silicate porous bioceramics using a non-sacrificial preceramic polymer binder, Biofabrication 7 (2015) 025008.
[11] J.S. Fernandes, P. Gentile, R. Moorehead, A. Crawford, C.A. Miller, R.A. Pires, P.V. Hatton, R.L. Reis, Design and properties of novel substituted borosilicate bioactive glasses and their glass-ceramic derivatives, Cryst. Growth Des. 16 (2016) 3731–3740.
[12] H. Elsayed, H. Javed, A.G. Sabato, F. Smeacetto, E. Bernardo, Novel glass-ceramic SOFC sealants from glass powders and a reactive silicone binder, J. Eur. Ceram. Soc. 38 (2018) 4245–4251.
[13] H. Elsayed, M. Picicco, A. Dasan, J. Kraxner, D. Galusek, E. Bernardo, Glass powders and reactive silicone binder: interactions and application to additive manufacturing of bioactive glass-ceramic scaffolds, Ceram. Int. 45 (2019) 13740–13746.
[14] S. Hillier, Accurate quantitative analysis of clay and other minerals in sandstones by XRD: comparison of a Rietveld and a reference intensity ratio (RIR) method and the importance of sample preparation, Clay Miner. 35 (2000) 291–302.
[15] A. Ray, A.N. Tiwari, Compaction and sintering behaviour of glass-alumina composites, Mater. Chem. Phys. 67 (2001) 220–225.
[16] L. Fiocco, S. Li, M.M. Stevens, E. Bernardo, J.R. Jones, Biocompatibility and bioactivity of porous polymer-derived Ca-Mg silicate ceramics, Acta Biomater. 50 (2017) 56–67.
[17] W. Höland, G. Beall, Glass-Ceramic Technology, The American Ceramic Society, Westerville OH, USA, 2002.
[18] G. Kaur, V. Kumar, F. Baino, J.C. Mauro, G. Pickrell, I. Evans, O. Bretcanu, Mechanical properties of bioactive glasses, ceramics, glass-ceramics and composites: state-of-the-art review and future challenges, Mater. Sci. Eng. C 104 (2019) 109895.
[19] M.C. Crovace, M.T. Souza, C.R. Chinaglia, O. Peitl, E.D. Zanotto, Biosilicate®—a multipurpose, highly bioactive glass-ceramic. In vitro, in vivo and clinical trials, J. Non-Cryst. Sol. 432 (2016) 90–110.